論文 한국공작기계학회지 제 7 권 제 1 호 1998. 2.
Journal of the Korean Society of Machine Tool Engineers

A New Approach to Moving Obstacle Avoidance Problem of a Mobile Robot

고 낙 용*, 최 정 상**

Nak Yong Ko*, Jung-Sang Choi**

Abstract

This paper presents a new solution approach to moving obstacle avoidance problem of a mobile robot. A new concept avoidability measure(AVM) is defined to describe the state of a pair of a robot and an obstacle regarding the collision between them. As an AVM, virtual distance function(VDF) is derived as a function of the distance from the obstacle to the robot and outward speed of the obstacle relative to the robot. By keeping the virtual distance above some positive limit value, the robot avoids the obstacle. In terms of the VDF, an artificial potential field is constructed to repel the robot away from the obstacle and to attract the robot toward a goal location. At every sampling time, the artificial potential field is updated and the force driving the robot is derived from the gradient of the artificial potential field. The suggested algorithm drives the robot to avoid moving obstacles in real time. Since the algorithm considers the mobility of the obstacle as well as the distance, it is effective for moving obstacle avoidance. Some simulation studies show the effectiveness of the proposed approach.

Keywords : Avoidability Measure, Virtual Distance Function, Moving Obstacle Avoidance, Mobility of Obstacles

1. Introduction

A moving obstacle avoidance problem is to plan and control the robot motion from an initial to a goal location avoiding moving obstacles. A robot usually works in a workspace with obstacles such as other robots, work pieces, machines, and workers. The robot should avoid the collision

* 조선대학교 제어계측공학과
** 조선대학교 산업공학과

※ This study was supported by Factory Automation Center for Parts of Vehicles(FACPOV) in Chosun University, Kwangju, Korea. FACPOV is designed as a regional research center of Korea Science and Engineering Foundation(KOSEF) and operated by Chosun University.

with them. The obstacles often move and change their shapes as well. So, time-varying obstacle avoidance is one of the main issues in robot motion planning. Especially, real-time obstacle avoidance is vital for robot motion in an unknown environment. This paper focuses on real-time moving obstacle avoidance. However, it's hard to find out a versatile solution method generating a collision-free trajectory for general problems in real-time. The main clue to solve the real-time moving obstacle avoidance problem is how to deal with the mobility of obstacles.

In some solution approaches[1-3], probabilistic models are used to describe the dynamic behavior of obstacles. In [1], the speed and the direction of a moving obstacle are modeled as random walk processes; and an optimization method is provided for the acceleration and deceleration of the vehicle. In [2], a stochastic motion-control algorithm based on a hidden Markov model is developed. Sharma[3] proposed a probabilistic model that represents the robot's dynamic behavior in response to collision alarms that have Poisson distribution, and safety rules that assume that some regions are safe.

Another approach used a space-time concept[4-6]. Space-time is constructed from a space by adding an extra time dimension to the space. In the space-time space, a time-varying obstacle is converted to a stationary obstacle. Thus, motion planning for time-varying obstacle avoidance is reduced to path planning for stationary obstacle avoidance in the space-time space. Though this approach mainly concerns off-line obstacle avoidance, it can be extended for real-time moving obstacle avoidance.

For real-time obstacle avoidance, Borenstein and Koren[7,8] constructed VFF(Virtual Force Field)[7] and VFH(Vector Field Histogram)[8] using information from ultrasonic sensors. Though this approach reduces the effect of sensor noise and drives the robot through a collision-free path, it has some difficulty in dealing with the mobility of moving obstacles in a dynamically changing environment.

In many of the previous researches for obstacle avoidance, only stationary obstacles are considered. In some cases stationary obstacle avoidance method is adopted for moving obstacle avoidance. Since the mobility of moving obstacles is not considered, these methods cannot steer the robot in response to the motion of moving obstacles and are not adequate for reactive motion. In this paper, we propose a new approach for real-time moving obstacle avoidance considering the mobility of moving obstacles. We introduce a new concept of avoidability measure(AVM). AVM is inversely proportional to the possibility that the robot collides with an obstacle. So, it measures how easily the robot can avoid an obstacle. As an AVM, we define virtual distance function(VDF), which associates the distance between the robot and an obstacle with the relative motion of the obstacle with respect to the robot. By keeping the virtual distance above some positive limit value, the robot avoids the obstacle. For simplicity, this work uses artificial potential field to maintain the VDF above the safe limit value. At each sampling time, an artificial potential is constructed in terms of the VDF. The robot moves according to the repulsive and attractive force induced by the artificial potential. The suggested algorithm drives the robot to avoid moving obstacles in real-time. Since the AVM and VDF consider the mobility of the obstacles as well as the distances, the proposed algorithm is effective for moving obstacle avoidance. Some simulation studies show the effectiveness of the proposed approach for moving obstacle avoidance.

We begin with problem formulation in section 2. The definition on AVM and VDF follows in section 3. VDF is a function of two variables: the distance from an obstacle to the robot and the

outward speed of the obstacle. In section 4, a collision-free motion planning method using VDF-based artificial potential field is presented. Some computer simulations show the effectiveness of the proposed method in section 5. Finally, we present a few concluding remarks in section 6.

2. Problem Formulation

We use the following nomenclature in solving the moving obstacle avoidance problem.

$\boldsymbol{P}=(x, y)$
a point in 2-dimensional space

$\boldsymbol{P}_r(t)=(x_r(t), y_r(t))$
position of the robot at time t

m mass of the robot

$\boldsymbol{P}_o(t)=(x_o(t), y_o(t))$
position of the obstacle at time t

r_o radius of an obstacle

$\boldsymbol{P}_{r,s}=(x_{r,s}, y_{r,s})$
initial location of the robot motion

$\boldsymbol{P}_{r,g}=(x_{r,g}, y_{r,g})$
goal location of the robot motion

t_i the i-th sampling time

Using the above nomenclature, the moving obstacle avoidance problem is formulated as the followings.

〔Moving obstacle avoidance problem〕

Given the position $\boldsymbol{P}_o(t_i)$ and the velocity $\dot{\boldsymbol{P}}_o(t_i)$ of an obstacle at every sampling time $t_i(i=0,1,2,\cdots)$ in 2-dimensional space, plan and control the robot motion from the initial location $\boldsymbol{P}_{r,s}$ to the goal location $\boldsymbol{P}_{r,g}$ avoiding the moving obstacle.

In our problem, the robot is assumed to be a point robot, and the obstacle be circular with the radius r_o.

3. Avoidability Measure and Virtual Distance Function

For stationary obstacle avoidance, it is sufficient to consider only the positions of the robot and obstacles. On the other hand, the mobility of the obstacles relative to the robot greatly influences the collision-free robot trajectory in moving obstacle avoidance. To consider the obstacle mobility in motion planning, we define the AVM in the following.

3.1 Avoidability Measure(AVM)

The distance between a robot and an obstacle can be used for detection of collision between them. The possibility of collision can be measured by the distance and the outward(or inward) speed of the obstacle relative to the robot. In other words, the distance and outward speed determine the possibility of collision avoidance. Thus, we select the distance and the outward speed as the state variables describing the possibility of collision avoidance. AVM is defined as a function of the two state variables in the following.

Definition : Avoidability measure(AVM) at time t is a function of the distance $d_{o,r}(t)$ and the outward speed $v_{o,r}(t)$, satisfying the following conditions.

(Condition 1) AVM increases as the distance $d_{o,r}(t)$ increases.

(Condition 2) AVM increases as the outward speed $v_{o,r}(t)$ increases.

where the distance $d_{o,r}(t)$ and outward speed $v_{o,r}(t)$ are defined as

$$d_{o,r}(t) = \| \boldsymbol{P}_o(t) - \boldsymbol{P}_r(t) \| - r_o \quad (1)$$

$$v_{o,r}(t) = \dot{\boldsymbol{P}}_o(t) \cdot \frac{\boldsymbol{P}_o(t) - \boldsymbol{P}_r(t)}{\| \boldsymbol{P}_o(t) - \boldsymbol{P}_r(t) \|} . \quad (2)$$

In the Definition, $v_{o,r}(t)$ is the projection of the obstacle velocity on the unit vector from the robot to the obstacle. So, it increases as the obstacle moves away from the robot and it becomes negative if the obstacle approaches to the robot; that is, it reflects the obstacle motion relative to the robot. In terms of the AVM, obstacle avoidance problem becomes to plan the robot motion keeping the AVM above a safe limit value to guarantee collision-free motion. For motion planning, our work uses virtual distance function as an AVM.

3.2 Virtual Distance Function(VDF)

There exist infinite number of functions satisfying the conditions for AVM. To calculate the driving force for a robot by numerical method, we propose a function called VDF for the AVM as

$$vd_{o,r}(d_{o,r}(t), v_{o,r}(t)) = \frac{\alpha}{\beta - v_{o,r}(t)} \cdot d_{o,r}(t) \quad (3)$$

where

$$\alpha > 0, \ \beta > \max\{ | v_{o,r}(t) | \} > 0, \ (\alpha, \beta \in \mathbf{R}). \quad (4)$$

We abbreviate $vd_{o,r}(d_{o,r}(t), v_{o,r}(t))$ as $vd_{o,r}(t)$ in the following. The $vd_{o,r}(t)$ increases as $d_{o,r}(t)$ or $v_{o,r}(t)$ increases; so, it satisfies the conditions for AVM. We set the robot to begin avoidance motion when $vd_{o,r}(t)$ decreases to a certain value.

In equation (3), as β increases, the less the $v_{o,r}(t)$ influences $vd_{o,r}(t)$; so, the distance has more influences on the collision-free trajectory than the outward speed does. On the contrary, too small β may result in too sensitive trajectory change in response to the obstacle motion. The α scales up or down the virtual distance $vd_{o,r}(t)$. If $v_{o,r}(t) = 0$, that is, there is no obstacle motion in the direction of the line $\overline{\boldsymbol{P}_o(t)\ \boldsymbol{P}_r(t)}$ or the obstacle is stationary, then $vd_{o,r}(t) = (\alpha/\beta) d_{o,r}(t)$. In this case, $vd_{o,r}(t)$ is proportional to the real distance $d_{o,r}(t)$, with the constant ratio α/β. Since the robot begins avoidance motion when $vd_{o,r}(t)$ decreases to a certain value, the robot begins avoidance motion far apart from the obstacle if $\alpha < \beta$; and the robot begins avoidance motion in the vicinity of the obstacle if $\alpha > \beta$. The α and β should be determined considering the aspects described in the above.

With the conditions of inequality (4), $vd_{o,r}(t) > 0$ if and only if $d_{o,r}(t) > 0$. Thus, the condition for collision avoidance is

$$vd_{o,r}(t) > 0, \ t \geq t_0. \quad (5)$$

In terms of the $vd_{o,r}(t)$, the moving obstacle avoidance problem becomes to plan and control the robot trajectory $\boldsymbol{P}_r(t)$, from $\boldsymbol{P}_{r,s}$ to $\boldsymbol{P}_{r,g}$, satisfying the condition of the inequality (5).

4. Moving Obstacle Avoidance

Methods of keeping the virtual distance above some positive limit value becomes moving obstacle avoidance method. Our work uses an artificial potential field to keep $vd_{o,r}(t) > 0$, for simplicity.

4.1 Artificial Potential Field in Terms of VDF

An artificial potential field is a field of forces where obstacles are repulsive surfaces against the robot, and the goal location is an attractive pole to the robot[9-13]. The artificial potential field

drives the robot through a collision-free trajectory to the goal location. Among many potential fields proposed, we adapt the potential field proposed by Khatib[9]. Since the potential field by Khatib[9] doesn't consider the movement of obstacles, it is not adequate for moving obstacle avoidance. We modify it using the VDF to construct the VDF based potential field. The potential field value at a location $\boldsymbol{P}$, $U_{art}(\boldsymbol{P}, \boldsymbol{P}_o(t), \boldsymbol{P}_{r,g})$ is defined as

$$U_{art}(\boldsymbol{P}, \boldsymbol{P}_o(t), \boldsymbol{P}_{r,g}) = U_o(\boldsymbol{P}, \boldsymbol{P}_o(t)) + U_g(\boldsymbol{P}, \boldsymbol{P}_{r,g}) \tag{6}$$

where

$$U_o(\boldsymbol{P}_r(t), \boldsymbol{P}_o(t)) = \begin{cases} \frac{1}{2}\eta\left(\frac{1}{vd_{o,r}(t)} - \frac{1}{\varepsilon_{vd}}\right)^2, & \text{if } vd_{o,r}(t) \le \varepsilon_{vd} \\ 0, & \text{if } vd_{o,r}(t) > \varepsilon_{vd}, (\varepsilon_{vd} > 0) \end{cases} \tag{7}$$

and

$$U_g(\boldsymbol{P}, \boldsymbol{P}_{r,g}) = \frac{1}{2}\zeta \| \boldsymbol{P} - \boldsymbol{P}_{r,g} \|^2. \tag{8}$$

$U_o(\boldsymbol{P}, \boldsymbol{P}_o(t))$ is the repulsive potential field inducing repulsive force from the obstacle at the location $\boldsymbol{P}_o(t)$, and $U_g(\boldsymbol{P}, \boldsymbol{P}_{r,g})$ is the attractive potential field inducing attractive force toward the goal location $\boldsymbol{P}_{r,g}$. In equation (7), ε_{vd} represents the limit virtual distance of the potential field influence, and $vd_{o,p}(t)$ is the virtual distance from the location $\boldsymbol{P}$ to $\boldsymbol{P}_o(t)$. As ε_{vd} increases, the $U_o(\boldsymbol{P}, \boldsymbol{P}_o(t))$ influences larger range, thus the robot begins avoidance motion farther apart from the obstacle. The η and ζ are constant coefficients for repulsive and attractive potential field respectively.

The force on the robot induced from the potential field is

$$\begin{aligned} \boldsymbol{F}_{art}(\boldsymbol{P}, \boldsymbol{P}_o(t), \boldsymbol{P}_{r,g}) &= -\nabla U_{art}(\boldsymbol{P}, \boldsymbol{P}_o(t), \boldsymbol{P}_{r,g}) \\ &= -\nabla U_o(\boldsymbol{P}, \boldsymbol{P}_o(t)) - \nabla U_g(\boldsymbol{P}, \boldsymbol{P}_{r,g}) \\ &= \boldsymbol{F}_o(\boldsymbol{P}, \boldsymbol{P}_o(t)) + \boldsymbol{F}_g(\boldsymbol{P}, \boldsymbol{P}_{r,g}). \end{aligned} \tag{9}$$

Hereafter, we abbreviate $\boldsymbol{F}_{art}(\boldsymbol{P}, \boldsymbol{P}_o(t), \boldsymbol{P}_{r,g})$ as $\boldsymbol{F}_{art}(\boldsymbol{P})$. The repulsive force $\boldsymbol{F}_o(\boldsymbol{P}, \boldsymbol{P}_o(t))$ increases as the robot approaches to the obstacle, and the attractive force $\boldsymbol{F}_g(\boldsymbol{P}, \boldsymbol{P}_{r,g})$ decreases as the robot approaches to the goal location. So, $\boldsymbol{F}_{art}(\boldsymbol{P}_r(t))$ drives the robot at location $\boldsymbol{P}_r(t)$ to the goal location through a collision-free path. However, $\boldsymbol{F}_{art}(\boldsymbol{P}_r(t))$ may drive the robot out of the robot's motion capability. In this case, $\boldsymbol{F}_{art}(\boldsymbol{P}_r(t))$ is scaled down to get the driving force, as will be explained in the following section.

4.2 Algorithm for Moving Obstacle Avoidance

The robot moves according to the commands issued at every sampling time t_i, $i = 0, 1, 2, \cdots$. At every sampling time t_i, the position and the velocity of an obstacle are sensed; and then the artificial force $\boldsymbol{F}_{art}(\boldsymbol{P}_r(t_i))$ is calculated by the equations (6)-(9). From the force $\boldsymbol{F}_{art}(\boldsymbol{P}_r(t_i))$, the force driving the robot till the next sampling time t_{i+1} is obtained.

For the i-th sampling period from t_i to t_{i+1}, the robot moves under the influence of the inertial force at time t_i as well as the artificial force $\boldsymbol{F}_{art}(\boldsymbol{P}_r(t_i))$. Meanwhile, the robot motion is subject to physical actuator force limits; that is, $\| \ddot{\boldsymbol{P}}_r(t) \|$ is constrained by the some acceleration limit, and $\| \dot{\boldsymbol{P}}_r(t) \|$ is constrained by some velocity limit. In the followings, the force driving the robot is derived from $\boldsymbol{F}_{art}(\boldsymbol{P}_r(t_i))$, considering the inertial force, acceleration

constraint, and the velocity constraint.

Combining the inertial force $m\,\tilde{P}_r(t_i)$ and artificial force $F_{art}(P_r(t_i))$, the resultant force $F_{comb}(t)$ is expressed as

$$F_{comb}(t) = m\,\tilde{P}_r(t_i) + F_{art}(P_r(t_i)), \quad t\in(t_i, t_{i+1}]. \tag{10}$$

The acceleration due to the $F_{comb}(t)$ is

$$\tilde{P}_r(t) = \frac{F_{comb}(t)}{m} = \tilde{P}_r(t_i) + \frac{F_{art}(P_r(t_i))}{m}, \quad t\in(t_i, t_{i+1}]. \tag{11}$$

If we set the acceleration limit as $a_{r,max}$, then $\tilde{P}_r(t)$ should be adjusted to satisfy the inequality (12).

$$\| \tilde{P}_r(t) \| = \left\| \tilde{P}_r(t_i) + \frac{F_{art}(P_r(t_i))}{m} \right\| \le a_{r,max}, \quad t\in(t_i, t_{i+1}] \tag{12}$$

To satisfy the inequality (12), $F_{art}(P_r(t_i))$ is scaled down as the $F_{acc}(P_r(t_i))$ of the equation (13).

$$F_{acc}(P_r(t_i)) = \max\left\{k\cdot F_{art}(P_r(t_i)) \;\middle|\; 0\le k\le 1, \left\| \tilde{P}_r(t_i) + \frac{k\cdot F_{art}(P_r(t_i))}{m} \right\| \le a_{r,max}\right\}, \quad t\in(t_i, t_{i+1}] \tag{13}$$

In (13), $F_{art}(P_r(t_i))$ is scaled down to the $F_{acc}(P_r(t_i))$ with the coefficient k, if the acceleration exerted by the force $F_{comb}(t)$ exceeds the acceleration limit $a_{r,max}$. With the force $F_{acc}(P_r(t_i))$, the robot moves with the velocity

$$\dot{P}_r(t) = \dot{P}_r(t_i) + (t-t_i)\cdot a_{acc}(t_i), \quad t\in(t_i, t_{i+1}]. \tag{14}$$

where

$$a_{acc}(t_i) = \tilde{P}_r(t_i) + \frac{F_{acc}(P_r(t_i))}{m} \tag{15}$$

Now, if we set the velocity limit as $v_{r,max}$, then $\dot{P}_r(t)$ should be adjusted to satisfy the inequality (16).

$$\| \dot{P}_r(t) \| = \left\| \dot{P}_r(t_i) + (t-t_i)\cdot a_{acc}(t_i) \right\| \le v_{r,max}, \quad t\in(t_i, t_{i+1}] \tag{16}$$

Therefore, if $\| \dot{P}_r(t) \| > v_{r,max}$ at time $t\ge t_v\,(t_v\in(t_i, t_{i+1}])$, $\dot{P}_r(t)$ should be constrained to $\dot{P}_r(t_v)$ for the time $t\in(t_v, t_{i+1}]$, as expressed in (17).

$$\dot{P}_r(t) = (\dot{x}_r(t),\ \dot{y}_r(t)) = \begin{cases} \dot{P}_r(t_i) + (t-t_i)\cdot a_{acc}(t_i), & t_i < t \le t_v \\ \dot{P}_r(t_i) + (t_v-t_i)\cdot a_{acc}(t_i), & t_v < t \le t_{i+1} \end{cases} \tag{17}$$

where, t_v satisfies

$$\left\| \dot{P}_r(t_i) + (t_v-t_i)\cdot a_{acc}(t_i) \right\| = v_{r,max} \tag{18}$$

Through the equations (14) and (18), the acceleration on robot motion satisfying both constraints is obtained as the $a_{drive}(t)$ of the equation (19).

$$a_{drive}(t) = \begin{cases} a_{acc}(t_i), & t_i < t \le t_v \\ 0, & t_v < t \le t_{i+1} \end{cases} \tag{19}$$

where

$$\left\| \dot{P}_r(t_i) + (t_v-t_i)\cdot a_{acc}(t_i) \right\| = v_{r,max}$$

As a result, the driving force for robot motion, $F_{drive}(t)$ is determined to get the acceleration of

(19) as the equation (20).

$$\boldsymbol{F}_{drive}(t)=\begin{cases}\boldsymbol{F}_{acc}(t), & t_i<t\le t_v\\ -m\ \ddot{\boldsymbol{P}}_r(t_i), & t_v<t\le t_{i+1}\end{cases}$$
$$\text{where}\quad \left\| \dot{\boldsymbol{P}}_r(t_i)+(t_v-t_i)\cdot \boldsymbol{a}_{acc}(t_i)\right\| = v_{r,max} \tag{20}$$

The robot driven by the force of (20) reaches to the location $\boldsymbol{P}_r(t_{i+1})$ at time $t=t_{i+1}$, as shown in (21).

$$\begin{aligned}\boldsymbol{P}_r(t_{i+1}) &= (x_r(t_{i+1}),\ y_r(t_{i+1}))\\ &= \Big(x_r(t_i)+\int_{\tau=t_i}^{\tau=t_{i+1}} \dot{x}_r(\tau)\,d\tau,\ y_r(t_i)\\ &\quad +\int_{\tau=t_i}^{\tau=t_{i+1}} \dot{y}_r(\tau)\,d\tau\Big)\end{aligned} \tag{21}$$

Summing up the above discussions results in the following moving obstacle avoidance procedure.

[Moving Obstacle Avoidance Procedure]

Step 0 : Set $i=0$.

Step 1 : Detect the $\boldsymbol{P}_o(t_i)$ and $\dot{\boldsymbol{P}}_o(t_i)$.

Step 2 : Calculate $vd_{o,r}(t_i)$ using the equation (3).

Step 3 : Calculate the $U_{art}(\boldsymbol{P}_r(t_i))$ using the equations (6)-(8).

Step 4 : Determine the force $\boldsymbol{F}_{drive}(t)$ using the equation (20), and drive the robot by the force.

Step 5 : If the robot collides with the obstacle at some time $t\in(t_i, t_{i+1}]$, then stop the robot motion and quit the procedure.

Step 6 : Test if the robot reaches to the goal location at time t_{i+1}.

(1) If it reaches to the goal location, quit the procedure.

(2) If it doesn't reach to the goal location, then set $i\leftarrow i+1$ and go to Step 1.

To test if the robot reaches to the goal location at time $t=t_{i+1}$, the following criterion is used.

$$\begin{aligned}&\| \boldsymbol{P}_r(t_k)-\boldsymbol{P}_{r,g}\| \le \varepsilon_d,\\ &for\ all\quad k=(i+1)-N,\cdots,i,i+1\end{aligned} \tag{22}$$

If the inequality (22) holds, the robot resides within the range of maximum distance ε_d from the goal location, for $N+1$ consecutive sampling times. Figure 1 depicts the procedure.

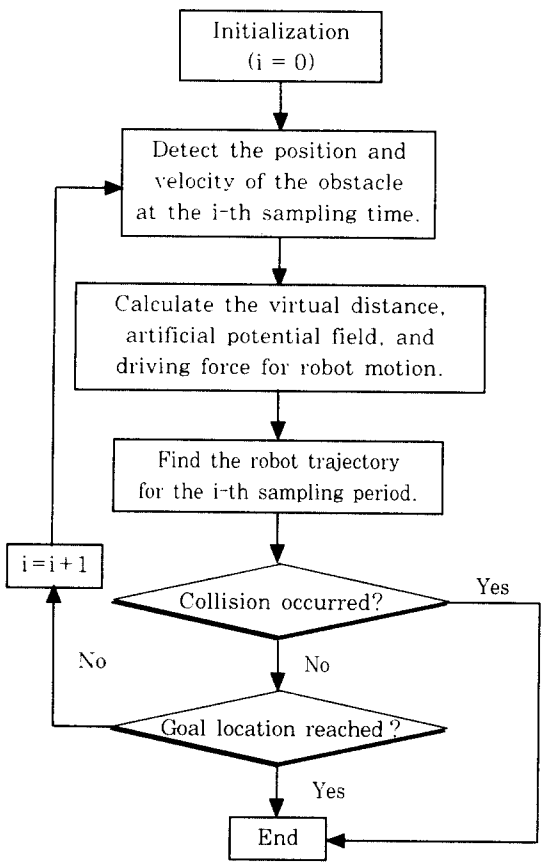

Fig 1. Flow diagram of the motion planning procedure.

5. Simulation Examples

The proposed method is applied for collision-free motion planning in seven different cases.

The first three cases show the robot trajectories avoiding a moving obstacle with three different obstacle velocities. In these cases, the obstacle moves through a straight line path with constant velocity. The last four cases show the robot trajectories avoiding three moving obstacles. In these cases, we compare the collision-free trajectories resulting from different values of the parameters α and β.

5.1 Conditions for Simulation

For the first three cases, the conditions are the same except for the velocity of the obstacle motion. The data common to all the three simulation studies are as the followings:

$$\boldsymbol{P}_{r,s}=(0,2)[cm], \quad \boldsymbol{P}_{r,g}=(80,-40)[cm],$$
$$m=0.1Kg, \quad r_o=5cm, \quad \boldsymbol{P}_o(t_0)=(55,3)[cm],$$
$$a_{r,max}=500cm/\sec^2, \quad \Delta t_i=0.1\sec(i=0,1,\cdots).$$

The parameters for virtual distance and artificial potential field are as the followings.

$$\alpha=5, \quad \beta=5, \quad \eta=1000, \quad \zeta=2, \quad \varepsilon_{vd}=40cm$$

The obstacle moves through a straight line path with constant velocity. Different obstacle velocity results in different collision-free trajectory of the robot. The velocities for the three cases are given as the followings.

(case 1)

$$\dot{\boldsymbol{P}}_o(t)=(-5,-10)[cm/\sec], \ for\ all\ t\geq t_0$$

(case 2)

$$\dot{\boldsymbol{P}}_o(t)=(-5,-11)[cm/\sec], \ for\ all\ t\geq t_0$$

(case 3)

$$\dot{\boldsymbol{P}}_o(t)=(-5,-14)[cm/\sec], \ for\ all\ t\geq t_0$$

Each case has y-directional speed different from the others.

For the last four cases, the obstacles move through arbitrary paths with time-varying velocities. The conditions for obstacles' motion are the same for the cases. And so are the values of η, ζ, and ε_{vd}. Only the values of the parameters α and β differ from case to case. The conditions common to these case studies are as the followings.

$$\boldsymbol{P}_{r,s}=(10,80)[cm], \quad \boldsymbol{P}_{r,g}=(180,70)[cm],$$
$$m=0.1\ \mathrm{Kg}, \quad r_o=2cm, \quad a_{r,max}=500cm/\sec^2,$$
$$\Delta t=0.1\sec(i=0,1,\cdots)$$
$$\eta=10^4, \quad \zeta=2, \quad \varepsilon_{vd}=40cm$$

In the cases 4 to 7, the values for α and β are selected as the Table 1.

Table 1. Values of α and β for the cases 4 to 7.

parameter	α	β
case 4	90.0	90.0
case 5	500.0	90.0
case 6	90.0	150.0
case 7	10^8	10^8

5.2 Simulation Results

The Figures 2-4 show the results for the cases 1-3. In case 1, the obstacle moves more slowly than the other cases. The robot begins avoidance motion from $t=t_{16}$, detours and moves forward before the obstacle reaches to the robot. The robot completes avoidance motion at $t=t_{26}$.

As the obstacle moves faster, the robot cannot go ahead of the obstacle. Only after the obstacle moves away, it passes over the obstacle path as in the cases 2 and 3. In case 2, as the obstacle approaches the robot's way, the robot moves back and forth six times from $t=t_{16}$ to $t=t_{29}$, and doesn't proceed until the obstacle passes away. It finally takes the back track of the obstacle. In

case 3, the robot detours slightly to the back of the obstacle.

In case 4, the robot avoids three moving obstacles with time-varying velocities as shown in Figure 5. In the case 5, as the parameter α increases from 90 to 500, virtual distance becomes larger than the real distance with the ratio of approximately 500/90. So, the robot doesn't begin avoidance motion until it approaches closer to the obstacles. Thus, as shown in Figure 6, the robot collides with the obstacle 1 at time $t = t_{14}$. As the β increases from 90 to 150, virtual distance becomes smaller than the real distance with the ratio of approximately 90/150. So, the robot begins avoidance motion far apart from the obstacles in case 6. As shown in Figure 7, the robot begins avoidance motion at time $t = t_8$, for obstacle 1. In addition, the robot trajectory changes more abruptly than does in the case 4. In case 7, α and β becomes extremely large compared with the outward speed of obstacle $v_{o,r}(t)$. In this case, $v_{o,r}(t)$ hardly influences the virtual distance. Therefore, virtual distance becomes real distance, and the proposed method becomes a conventional potential field method used for stationary obstacle avoidance. Figure 8 reveals that the robot trajectory doesn't respond to the approach of obstacle 3. Moreover, the robot makes an unnecessary detour after it passes away the obstacle 3 path already. This is because the potential field method based on real distance doesn't consider the mobility of obstacle at all.

As in the equation (7), the virtual distance is used in artificial potential field as distance value. So, the robot changes its trajectory in responseto the change of virtual distance instead of realdistance to obstacles. Figures 9-12 show the change of virtual distance for the cases 4-7 respectively. In case 5, the virtual distance between the robot and obstacle 1 becomes

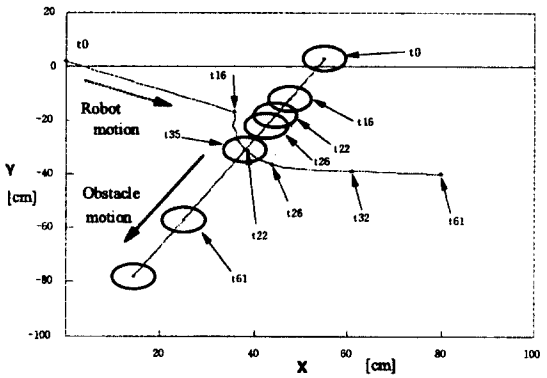

Fig 2. Collision avoidance motion for the case 1.

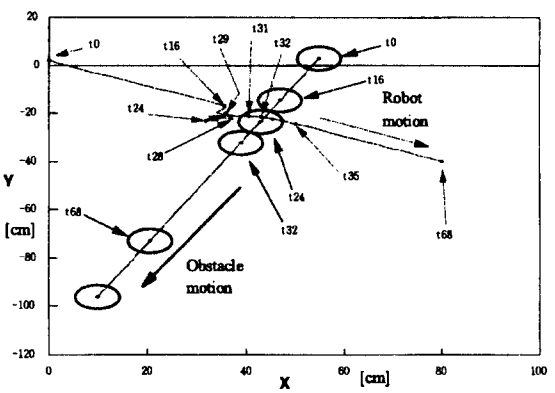

Fig 3. Collision avoidance motion for the case 2.

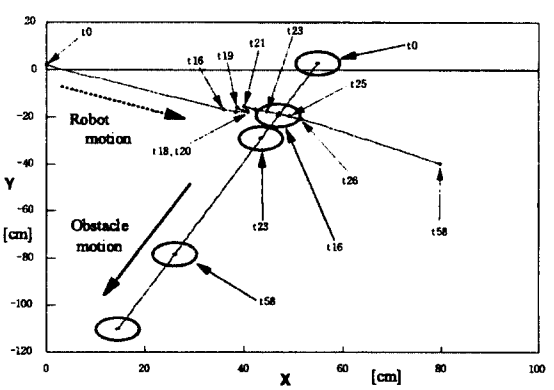

Fig 4. Collision avoidance motion for the case 3.

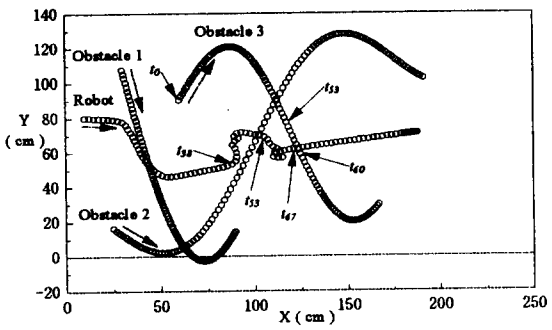

Fig 5. Collision avoidance motion for the case 4($\alpha=90$, $\beta=90$).

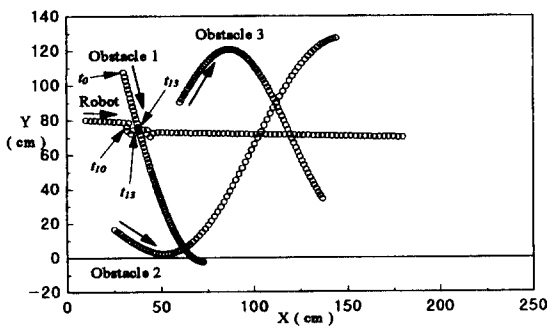

Fig 6. Collision avoidance motion for the case 5 ($\alpha=500$, $\beta=90$).

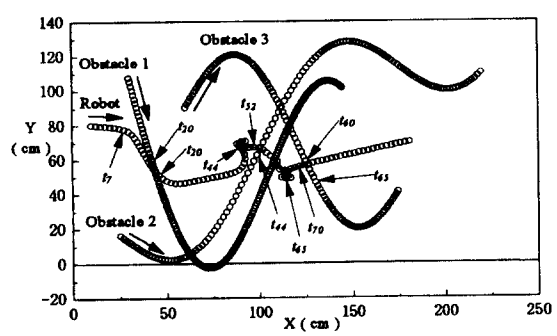

Fig 7. Collision avoidance motion for the case 6($\alpha=90$, $\beta=150$).

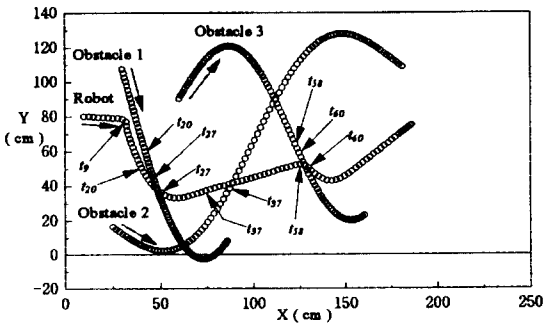

Fig 8. Collision avoidance motion for the case 7($\alpha=\beta=10^8$).

negative from the 14-th sampling time, and the robot collides with the obstacle 1. In case 4, as the obstacle 1 approaches to the robot, virtual distance becomes near zero though the real distance is greater than zero, so that the robot changes its trajectory to prevent collision. In this case, the values of α and β are set properly so that the virtual distances reflect the mobility of obstacles. Meanwhile, in case 7, the virtual distances keep larger value than in the case 4, even though the obstacles approach close to robot. So the robot doesn't respond to the approach of obstacles. This is because the values of α and β are too large, and the virtual distances doesn't consider the mobility of obstacles.

For collision-free robot motion planning, values for α, β, η, ξ, and ε_{vd} should be determined considering the discussions in sections 3.2 and 4.1 and the results of cases 4 to 7. Different state of the robot and obstacle requires different values for them. The selection of the values for them often requires some trial and error. The virtual distance also

Since potential field is used in calculating the driving force, some problems such as local minimum, oscillation in the corridor may arise.

However, as the obstacles move, the local minima also move and sometimes disappear. So, the local minima problem in the moving obstacle avoidance case is less severe than in the case of stationary obstacle avoidance. Also, these problems can be solved using some heuristics. Besides, another method not using the potential field can be used to maintain the virtual distance above safe limit value.

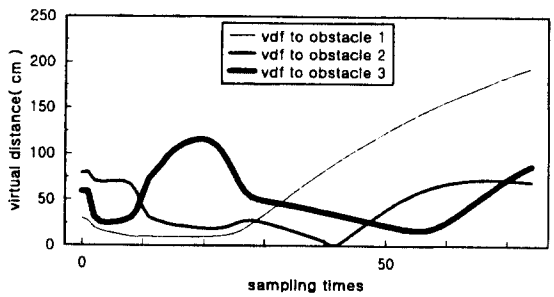

Fig 9. Virtual distances for the case 4 ($\alpha=90$, $\beta=90$).

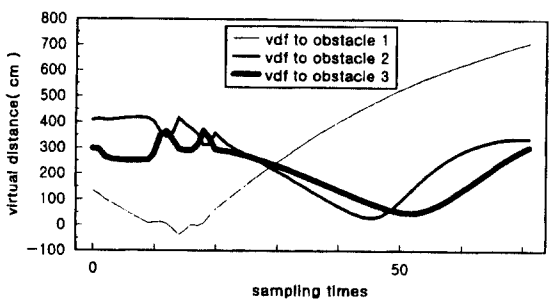

Fig 10. Virtual distances for the case 5 ($\alpha=500$, $\beta=90$).

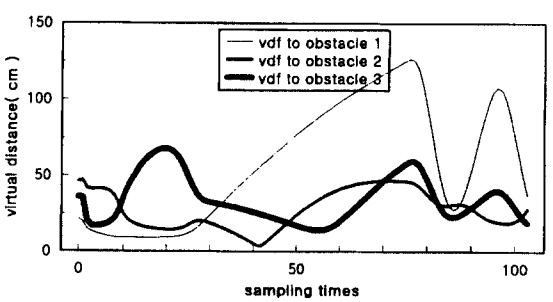

Fig 11. Virtual distances for the case 6 ($\alpha=90$, $\beta=150$).

6. Conclusions

A new method for real-time moving obstacle avoidance is proposed. It introduces AVM describing the status of the robot and obstacle in the viewpoint

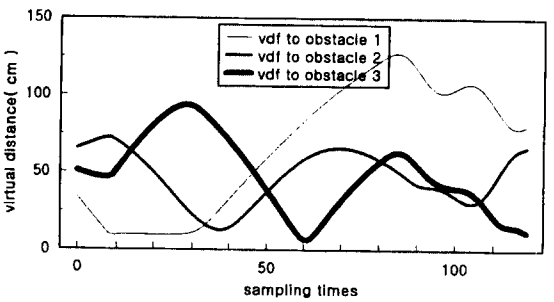

Fig 12. Virtual distances for the case 7 ($\alpha=\beta=10^8$).

of collision. As an AVM, the VDF is derived, and then used to construct artificial potential field for obstacle avoidance.

For real application of the proposed method, it is required to detect the obstacle location and velocity at every sampling time[14]. Thus, it is not applicable in cases where it is not possible to detect the location and velocity, or it takes long time to detect them. However, if the workspace is small enough to be covered by a frame of a camera, the location and velocity can be detected from visual information[15], and the AVM method can be applied. Also, the proposed method can be applied for collision-free motion coordination of multiple robots, because each robot can detect its location and velocity, and transmit them to another robots[16,17].

Since the AVM and VDF considers obstacle motion relative to the robot, the AVM based method is adequate for moving obstacle avoidance. As shown in the simulation results, it works as expected for various circumstances. It remains for further research to apply the method for real robot motion planning in an environment of multiple moving

obstacles with various path and trajectories.

Acknowledgements

This study was supported by Factory Automation Center for Parts of Vehicles(FACPOV) in Chosun University, Kwangju, Korea. FACPOV is designed as a regional research center of Korea Science and Engineering Foundation(KOSEF) and operated by Chosun University.

References

1. N.C.Griswold and J.Eem, "Control for mobile robots in the presence of moving objects," IEEE trans. Robotics and Automation, Vol.6, No.2, pp.263-268, April 1990.
2. Q.Zhu, "Hidden Markov model for dynamic obstacle avoidance of mobile robot navigation," IEEE trans. Robotics and Automation, Vol.7, No.3, pp.390-397, June 1991.
3. R.Sharma, "Locally efficient path planning in an uncertain, dynamic environment using a probabilistic model," IEEE trans. Robotics and Automation, Vol.8, No.1, pp.105-110, Feb.1992.
4. K.Fujimura and H.Samet, "A hierarchical strategy for path planning among moving obstacles," IEEE Trans. on Robotics and Automation, Vol. 5, No. 1, pp. 61-69, Feb. 1989.
5. M.Erdmann and T.Lozano-Pérez, "On multiple moving objects," in Proc. 1986 IEEE Int. Conf. Robotics Automat., pp.1419-1424, 1986.
6. C.L.Shih, T.T.Lee, and W.A.Gruver, "A unified approach for robot motion planning with moving polyhedral obstacles," IEEE Trans. Syst., Man, Cybern., Vol.20, No.4, pp.903-915, July/Aug. 1990.
7. J.Borenstein and Y.Koren, "Real-time obstacle avoidance for fast mobile robots," IEEE Trans. on System, Man, and Cybernetics, Vol. 19, No. 5, pp. 1179-1187, 1989.
8. J.Borenstein and Y.Koren, "The vector field histogram-fast obstacle avoidance for mobile robots," IEEE Trans. on Robotics and Automation, Vol. 7, No. 3, pp. 278-288, June 1991.
9. O.Khatib, "Real-time obstacle avoidance for manipulators and mobile robots," The Int. J. Robotics Research, Vol.5, No.1, pp.90-98, Spring 1986.
10. B.H.Krogh, "A generalized potential field approach to obstacle avoidance control," SME Conf. Proc., Robotics Research: The Next Five Years and Beyond, 1984.
11. R.Volpe and P.Khosla, "Manipulator control with superquadric artificial potential functions: Theory and experiments," IEEE Trans. on System, Man, and Cybernetics, Vol. 20, No. 6, pp.1423-1436, Nov./Dec. 1990.
12. Y.K.Hwang and N.Ahuja, "A potential field approach to path planning," IEEE Trans. on Robotics and Automation, Vol. 8, No.1, pp.23-32, Feb. 1992.
13. E.Rimon and D.E.Koditschek, "Exact robot navigation using artificial potential functions," IEEE Trans. on Robotics and Automation, Vol. 8, No.5, pp.501-518, Oct. 1992.
14. T.Aoki, T.Oka, T.Suzuki, and S.Okuma, "Acquisition of optimal action selection to avoid moving obstacles in autonomous mobile robot," in Proc. 1996 IEEE Int. Conf. on Robotics and Automation, pp.2055-2060, Minneapolis, Minnesota, April 1996.
15. Kan-Han Tan and M. Authony Lewis, "Virtual structures for high-precision cooperative mobile robot control," in Proc. 1996 International Conference on Intelligent Robots and Systems, pp.132-139, Osaka Japan, November 1996.
16. Y.Arai, S.Suzuki, S.Kotosaka, H.Asama, H.Kaetsu, and I.Endo, "Collision avoidance among multiple autonomous mobile robots using LOCISS," in Proc. 1996 IEEE Int. Conf. on Robotics and Automation, pp.2091-2096, Minneapolis, Minnesota, April 1996.

17. R.Kurazume, S.Hirose, S.Nagata, and N.Sashida, "Study on cooperative positioning system," in Proc. 1996 IEEE Int. Conf. on Robotics and Automation, pp.1421-1426, Minneapolis, Minnesota, April 1996.